ELSEVIER

Polymer 40 (1998) 1–11

polymer

Frustration and single crystal morphology of isotactic poly(2-vinylpyridine)

T. Okihara[a,b], L. Cartier[a], G.O.R. Alberda van Ekenstein[c], B. Lotz[a,*]

[a]*Institut Charles Sadron (CNRS-ULP), 6, rue Boussingault, 67083 Strasbourg, France*
[b]*Department of Applied Chemistry, Faculty of Engineering, Okayama University, 3-1-1 Tsushima, Okayama 700, Japan*
[c]*Department of Polymer Chemistry, State University of Groningen, Nijenborgh 16, 9747 AG Groningen, The Netherlands*

Received 17 December 1997; revised 25 February 1998; accepted 3 March 1998

Abstract

The crystal structure of isotactic poly(2-vinylpyridine) (iP2VP) established in 1977 by Puterman et al. is shown to conform to a recently proposed frustrated packing scheme which involves three isochiral three-fold helices packed in a trigonal unit-cell, and observed in a number of polymers and biopolymers. Single crystals of iP2VP grown from thin films at high temperature ($Tc \approx 200°C$) display highly unusual morphologies with six (100) growth sectors but a three-fold overall symmetry apparent through different lamellar thicknesses in adjacent growth sectors, and oblique growth facets of three of the sectors. These features are morphological manifestations of the frustration of the helix packing, and support the $P3_1$ or $P3_2$ space group of the unit-cell. The different lamellar thicknesses are mainly due to an isothermal thickening process, which has different impacts depending on the nature of the growth faces. Analysis of the growth features of frustrated structures can be of help when dealing with finer details of theories of polymer crystal growth.

Keywords: Crystal morphology; Isotactic poly(2-vinylpyridine); Isothermal thickening

1. Introduction

Isotactic poly(2-vinylpyridine) (iP2VP) is structurally very similar to isotactic polystyrene. It differs from the latter by substitution in position 2 of the aromatic ring of one CH unit by a nitrogen:

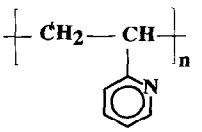

The crystallization kinetics of iP2VP have been investigated by van Ekenstein et al. [1] and the crystal structure determined by Puterman et al. [2] in 1977. The structure is highly original since it displays several features which had no equivalent in polymer science for nearly 20 years. It is based on a trigonal unit-cell with parameters $a = b = 15.49$ Å, $c = 6.56$ Å, space group $P3_1$ or $P3_2$ comprising three isochiral three-fold helices. In addition, the azimuthal setting of the helices on their axis is highly unconventional (cf. Fig. 4*a*). As discussed by Puterman et al. [2] the special combination of settings leads to a crystal structure in which identical helices have different environments.

The crystal structure of iP2VP is actually only one example of a recently uncovered family of crystal structures based on three three-fold helices packed in trigonal cells and which result in frustrated packings. The concept of frustration was introduced in materials science by Toulouse [3] to describe the mutual orientation of magnetic spins in antiferromagnetic systems. Frustration exists whenever vicinal requirements (e.g. antiparallelism of spins) is incompatible with packing requirements (e.g. close packed hexagonal, or Kagomé lattices) [4]. Frustration was introduced in polymer crystallography by Lotz et al. [5]. It is manifested by different azimuthal settings of isochiral three-fold helices packed in a trigonal unit-cell containing three chains. In addition to the present iP2VP structure, it has been observed for various *achiral* polymers: isotactic polypropylene in its metastable β modification (βiPP) [5–7] and syndiotactic polystyrene (sPS) in its α'' form [5]), and for various *chiral* polymers: poly(*tert*-butylethylene sulfide)

* Corresponding author.

0032-3861/98/$ - see front matter
PII: S0032-3861(98)00220-1

(PTBES) and biopolymers [8]: poly(L-hydroxyproline), triethylcellulose, etc.

Besides several specific characteristics of the diffraction pattern, frustrated polymer structures frequently display a highly original triangular single crystal morphology [8,9] which is a macroscopic manifestation of the fact that the front and back faces of any crystallographic plane have different topologies. This difference induces unequal 'front' and 'back' growth rates for (typically (100)) growth planes, and therefore results in the triangular, rather than hexagonal, single crystal morphology.

In the present paper, we present and analyse the morphology of melt grown single crystals of iP2VP already presented briefly in a paper on triangular single crystals [9]. Although the growth kinetics of iP2VP have been investigated in the past [1], no report exists on its single crystals. The latter are highly original: although we are dealing with a chiral but racemic polymer (as is iPP), they have a three-fold symmetry in spite of (nearly) hexagonal outline. They display additional features (different lamellar thicknesses for nominally equivalent growth sectors, oblique growth faces) which are further manifestations of frustration, and which suggest that present theories of polymer crystallization need to be adapted to account for the new crystallographic and growth features introduced by frustrated structures.

2. Experimental

2.1. Samples and sample preparation

The sample most often used in this study was produced as detailed in [1]. Its (viscometric) molecular weight is 112 000, and it has a 98% isotacticity index. Crystal growth is conducted in thin films. Amorphous thin films are produced by casting a 0.1% (w/v) solution in ethanol at 40°C. In view of the limited heat resistance of iP2VP, the crystallization process is carried under a nitrogen atmosphere (in a Mettler hot stage) and avoids melting and recrystallization: rather, it uses annealing of the amorphous polymer in the crystallization range ($\approx$ 200°C) with heating rates of 10°C/min. It was noticed that the concentration of single crystals can be monitored to some extent by adjusting the heating rate, i.e. by varying the time spent by the sample in the low temperature part of the crystallization range, where nucleation is more profuse. After selected crystallization times (usually 15 h), the sample is cooled to room temperature at $-$ 20°C/min. The uncrystallized material left in the film is dissolved away with warm (40–50°C) toluene.

The resulting thin film, in which the single crystals are now more readily apparent in optical microscopy (phase contrast), is shadowed with Pt/C, backed with a carbon film, floated off on water and picked up on electron microscope grids. Although iP2VP is soluble in most polar sovents, it is not in water, which facilitates greatly the transfer of the samples to the electron microscope support grids.

2.2. Techniques

The samples are investigated by optical microscopy in phase contrast, by electron microscopy and diffraction (with a Philips CM12 microscope equipped with a tilting stage). Unshadowed samples are examined by Atomic Force Microscopy (Nanoscope III, Digital Instruments, Santa Barbara, CA, USA) in the contact and tapping modes. Note that 'dry' conditions are required, given the high solubility of iP2VP in most polar as well as apolar solvents. Molecular modelling is performed on a Silicon Graphics Indigo 2 workstation, using the relevant Cerius [2] packages developed by Biosym-Molecular Simulations (Cambridge, UK and Waltham, MA, USA).

3. Results

Single crystals of iP2VP grown from thin molten films at 195–200°C are shown in Fig. 1, as observed by phase contrast optical microscopy. Contrary to crystals of other (mainly chiral) polymers with frustrated structures, they display a hexagonal outline rather than a triangular one [9]. Furthermore, the different optical densities of the various

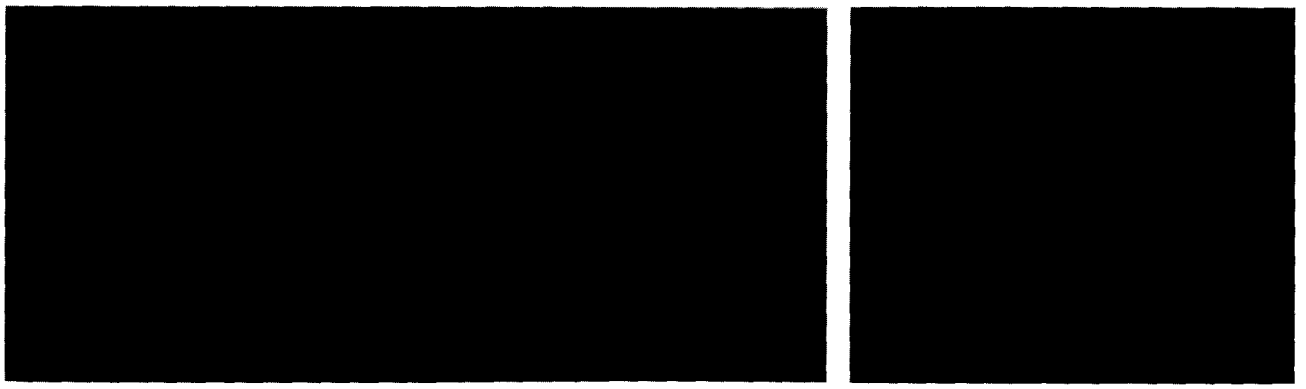

Fig. 1. Single crystals of iP2VP grown in thin film at 200°C as observed in phase contrast optical microscopy. Note the difference in optical density of the different growth sectors.

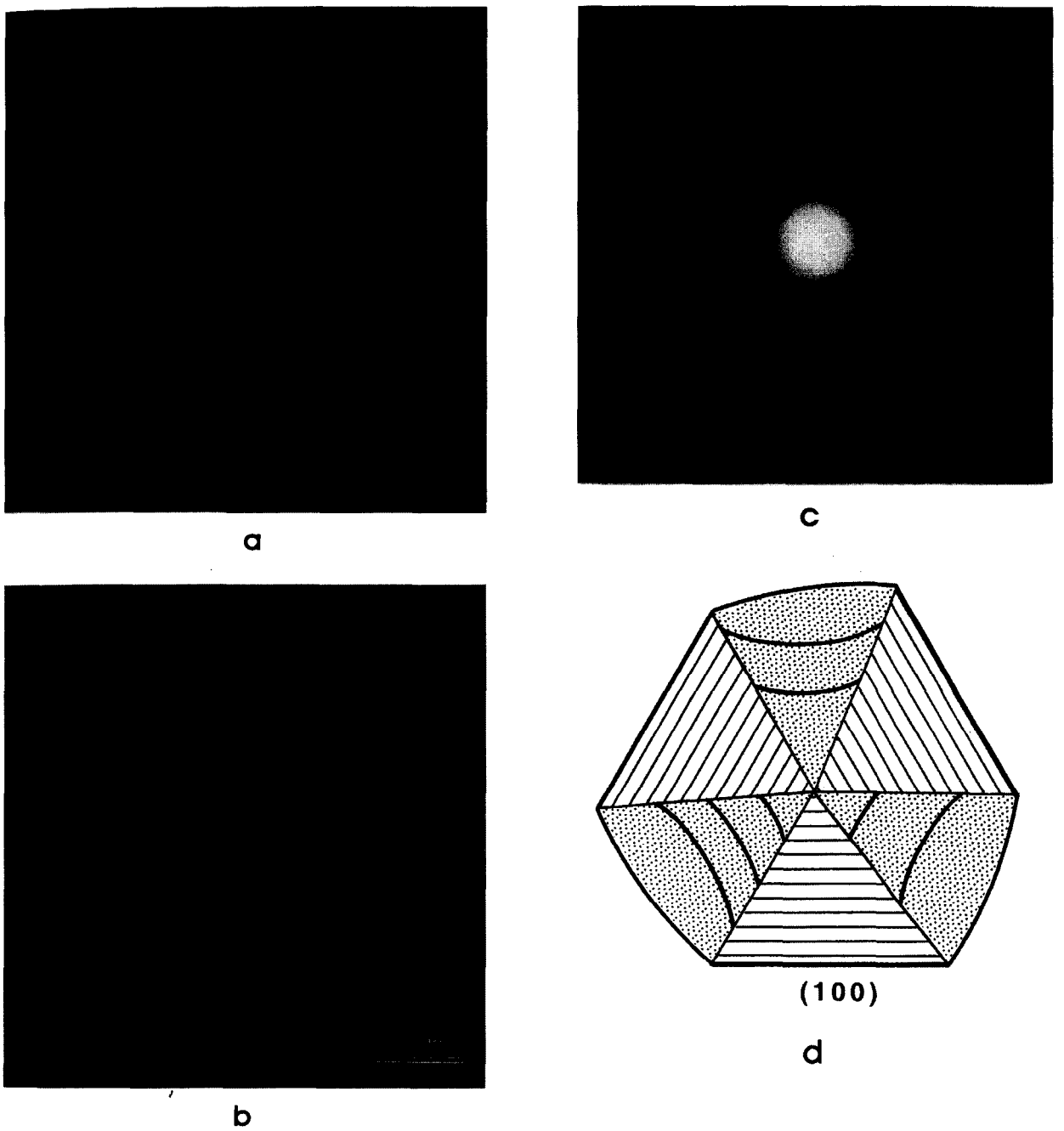

Fig. 2. (a) Single crystal of iP2VP grown in thin film at 190°C. Electron micrograph, Pt/C shadowing. (b) As in (a), with crystallization temperature 200°C. (c) electron diffraction pattern of single crystals as in (a) or (b) in proper relative orientation with the drawing of part (d). Note the characteristic pattern of frustrated structures. (d) Drawing of the crystals displayed in part (a), with indication of the thicker growth sectors (shaded) and the orientation of the crystallographic (100) growth planes.

growth sectors suggest that three sectors are thicker than their neighbours, with which they share common boundaries.

The above features are fully confirmed by examination of the single crystals in electron microscopy (Fig. 2*a* and *b*) and electron diffraction (Fig. 2*c*). The ED pattern confirms the trigonal symmetry of the unit-cell, as well as the cell dimensions determined by X-ray fibre diffraction by Puterman et al. [2].

The bright field electron micrographs reveal several features which have no precedent in polymer single crystal morphology. Indeed:

1. While the crystals have definitely a six-sided outline, they are not hexagonal. The relative orientation of the diffraction pattern and bright field leads to the analysis shown in Fig. 2*d*: three sectors are bound by well characterized (100) growth planes. The growth fronts of the

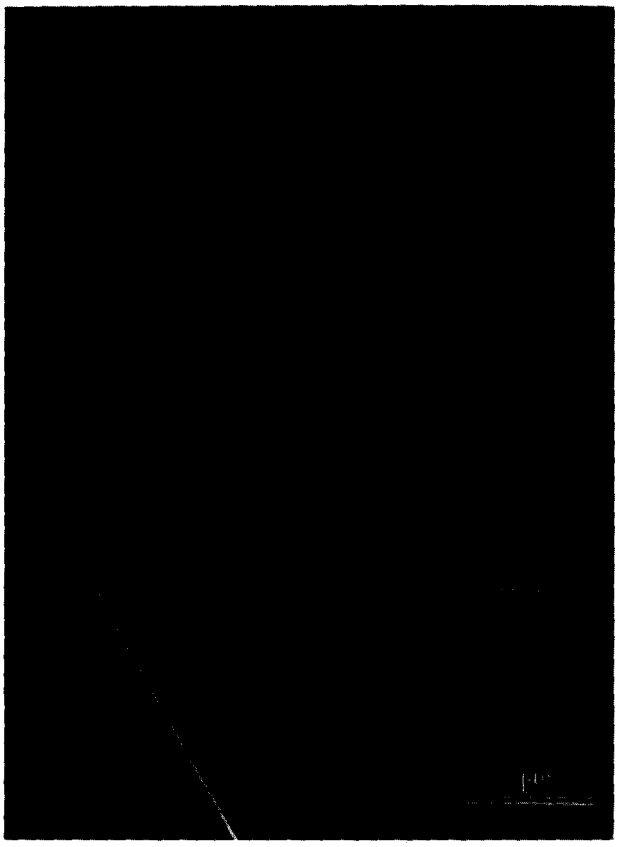

Fig. 3. Enlargment of part of a single crystal grown at 200°C, which displays different surface roughness in different growth sectors (growth sector boundaries are underlined). Note the smoothness and roughness of alternating sectors, as well as the development of large cracks, indicative of lamellar thickening. Electron micrograph, Pt/C shadowing.

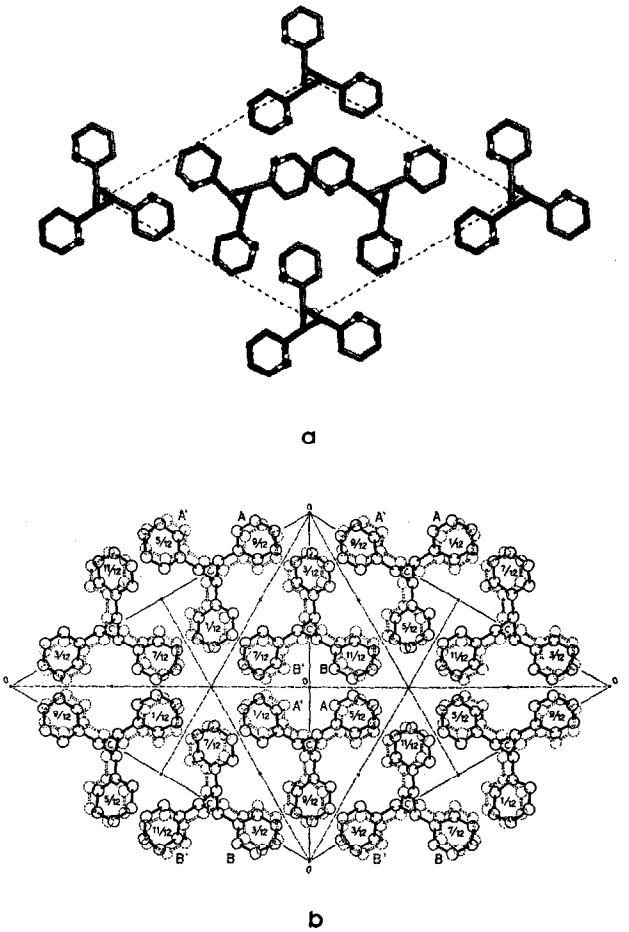

Fig. 4. (a) Crystal structure of iP2VP as determined by Puterman *et al.*[2] based on a trigonal unit-cell with three isochiral helices (space group $P3_1$). Nitrogen atoms in the aromatic ring are differentiated. Note the characteristic 'North–South–South' azimuthal settings of the three helices (characterized by the orientation of one of the aromatic side chains). (b) Crystal structure of isotactic polystyrene, which has a helical structure isoconformational to that of iP2VP. The structure, determined by Natta *et al.* is based on the packing and interdigitation of neighbouring antichiral helices.

other sectors are tilted to (100), but cannot be assigned any set of low Miller indices. They are certainly not the dense (110) planes, which would be tilted at 30° to (100) planes. Since growth planes with higher Miller indices are unlikely, we must consider that the growth front is indeed made of (100) growth planes, but that the tilt reflects some specific feature in that plane which results in different lateral growth rates on the growth front.

2. The unevenness of lateral growth rates in the growth sectors just inferred takes place with the same polarity for all three similar sectors. In other words, the crystal as a whole has a chirality: it is different if looked at from the top or from the bottom. This chirality is best illustrated by comparing the crystals displayed in Fig. 2*a* or *b* and *d*. If the tilted growth faces are considered as part of a spiral, the latter spirals outwards in an anticlockwise and a clockwise fashion in Fig. 2*a* and *d*, respectively.
3. The difference in lamellar thicknesses also help characterize the growth sectors. The sectors bound by 'flat' (100) growth faces are thinner, those bound by 'tilted' (100) faces are thicker. Lamellar thicknesses, measured by AFM, are $\approx$ 35 and 40 nm, respectively. AFM examination, supported by electron microscopy, also indicates that the thinner sectors have a very significant small scale surface roughness. This roughness does not arise from the cracks visible in the electron micrographs (cf. Fig. 2*a*) which delineate domains several micrometres across, but involves only very small patches, at most a few nanometres wide. This difference in surface roughness is best illustrated in the enlargment of Fig. 2*a* shown in Fig. 3, which displays 'spikes' protruding from the thinner sectors, with their characteristic, nearly triangular shadows.
4. The thicker growth sectors display, especially when grown at high temperature, a pattern of characteristic lines which suggest some form of corrugation (Fig. 2*b*). Unlike corrugated crystals of polyethylene however[10], the present lines are bent and do not correspond to well-defined crystallographic planes ((310) in PE). They have an overall 'inward' curvature, with its central part nearly parallel to (100) growth planes and the external parts oriented at an angle to the two growth sector boundaries.

4. Discussion

The unconventional morphological features of iP2VP single crystals described above turn out to be manifestations of its equally unconventional crystal structure based on a frustrated packing of helices (referred to in the following, for simplicity but not quite adequately, as 'frustrated structure'). It is therefore appropriate to present and discuss this crystal structure, and in particular its symmetry, since it is at the root of the observed morphology of the single crystals.

4.1. The crystal structure of isotactic poly(2-vinylpyridine)

4.1.1. The structure of iP2VP and comparison with the iPS structure

The trigonal crystal structure of iP2VP containing three chains determined by Puterman et al. [2] (Fig. 4*a*) is characterized by azimuthal settings which can be described, schematically, as North–South–South (NSS). Another version of the frustrated packing has been identified [11,12], with helix settings North–West–West (NWW), but which does not seem to apply for iP2VP. We have checked that the alternate NWW arrangement yields a significantly poorer match with the experimental *hk*0 electron diffraction pattern obtained from the single crystals (Fig. 2*c*).

One very minor modification to the structure seems however in order. It deals with the *c* axis repeat distance (6.56 Å) determined by Puterman et al. [2] which is a little shorter than that determined for isotactic polystyrene (iPS): 6.65 Å. These authors based this value on a reflection on the meridian, indexed as 003. It is however a characteristic of frustrated structures that the 103 reflection is stronger than 003. For an insufficiently oriented sample, this reflection may be considered to be meridional and indexed 003. Reassigning the 'meridional' reflection as 103 leads to a chain axis repeat distance of 6.65 Å, which is exactly that of iPS: the two polymers, which are both chiral but racemic, share the same helix conformation. They provide therefore an interesting pair which makes it possible to compare helix packing in frustrated and non-frustrated trigonal structures.

The crystal structures of iP2VP and of iPS are fundamentally different in spite of the isoconformation of their helices. iPS crystallizes in a trigonal unit-cell (Fig. 4*b*) with parameters $a = b = 21.9$ Å, $c = 6.5$ Å, space group R-3c[13]. The cell houses six chains, and is build up with bilayers in which helices of both hands alternate and interdigitate perfectly. The iPS crystal structure—as well as that of many other polymers, e.g. isotactic poly(1-butene) in its forms I and I′[14], or visotactic poly(vinylmethylether) [15]—takes full advantage of the presumably more favourable interdigitation of antichiral helices: indeed, the coordination number [16] (i.e. the number of structural units with which any one helix interacts) is three.

To the opposite, the frustrated packing scheme of iP2VP, although based also on a trigonal cell (but with $P3_1$ symmetry and three chains per cell) does not take advantage of the racemic nature of the chain, and of the possibility to form—and therefore pack—antichiral helices. In the frustrated packing, each helix interacts with six neighbours. A similar situation has been observed and analysed for βiPP [6,7], which is however metastable relative to the stable αiPP phase, the latter being made of antichiral helices with a coordination number of four [17].

A most surprising outcome of this comparison is that the crystal densities of iP2VP and iPS are virtually equal—within less than 1%. If anything, the crystal density of iP2VP is even a little higher than that of iPS, on account of the difference in atomic weight of a Nitrogen (14) and a CH (13). This near-identity of densities is best reflected by the $\sqrt{2}$ ratio between the *a* axis parameters of the unit cells of iPS and iP2VP (the former cell houses twice the number of helices as the latter). This result confirms that the frustrated packing of isochiral helices is as efficient a packing as that of antichiral helices, which is often considered to take better advantage of the 'complementarity' of antichiral helical shapes; further illustrations of this statement are provided by the comparison of crystal structures of chiral, and of stereocomplexes of polylactides [9] and of poly(propylene-carbon monoxide) [18].

Also, the present comparison suggests that the frustrated packing could be a plausible structural alternative for iPS, and, conversely, the antichiral one would be an alternative for iP2VP. On this basis, we have attempted to grow the alternative, 'lacking' phases of iPS and iP2VP using as a substrate single crystals of the other polymer—but with no success. This failure appears to be due to the different polarities of the two polymers: they phase separate in the thin film.

4.1.2. Space group of iP2VP and frustrated structures

Two features of the structure need to be underlined when analysing the morphology of single crystals: the exact space group assignment (in particular with respect to up–down orientation of chains), and the possibility of twinning.

The space group of iP2VP used by Puterman et al. [2] is $P3_1$ or $P3_2$ (depending on helix hand). This space group is characterized by three three-fold screw axes at positions (0,0), (1/3, 2/3) and (2/3, 1/3) in the *ab* plane. This is a standard space group for one chain unit-cells: the structural unit is a single monomer unit and the position and relative heights of the neighbour helices are related by three-fold screw axes. In frustrated structures, the same symmetry elements of the unit-cell generate three helices, which implies that the repeat unit is either made of three independent residues, or of a single helix made of three residues. Since these two possibilities have both been used in the past but yield significantly different unit-cell contents, it is of interest to analyse their structural consequences.

When defining three independent residues, each of the three-fold screw axes contributes to generate one helix, each one from a different structural unit. All the symmetry

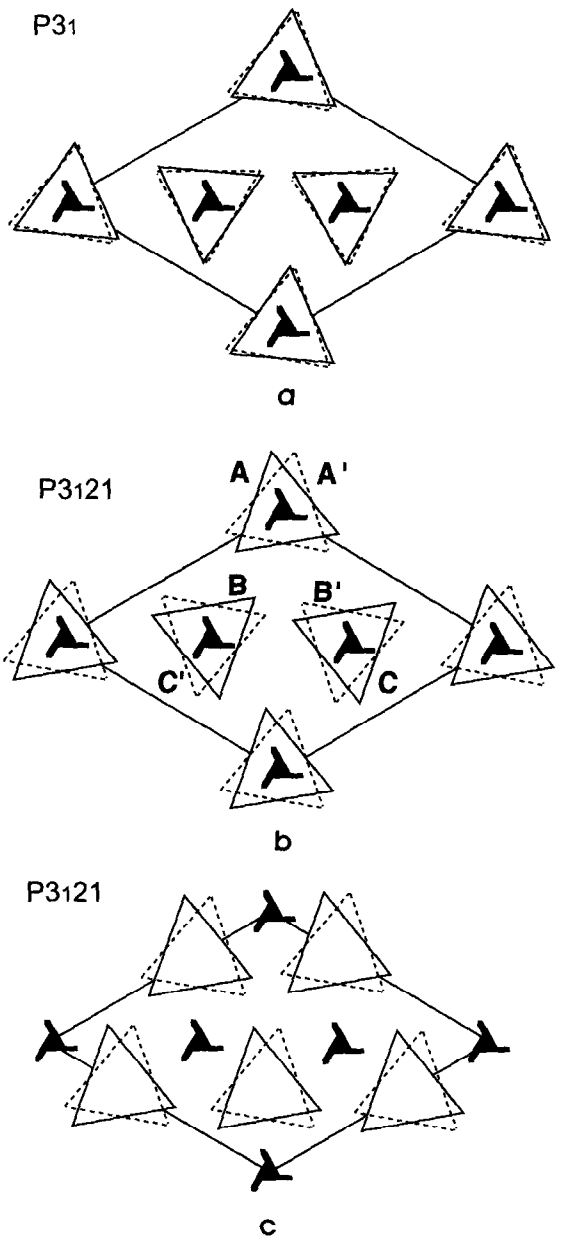

Fig. 5. Space groups used to describe crystal structures based on trigonal cells and including three helix sites: (a) $P3_1$ space group used by Puterman *et al.*[2] to describe the structure of iP2VP, and valid for frustrated structures. Note the helix axes centred on the screw axes, and the allowed different azimuthal settings of the helices, which may be kept for up (full lines) and down (dashed lines) pointing helices. (b) $P3_121$ space group with helix axes centred on screw axes. Note the special relationship between up and down (primed and shown in dashed lines) helices, and the different azimuthal settings allowed for the three helices. (c) $P3_121$ space group in which a full helix is defined as the structural repeat unit. The six helices generated (three up and three down) are linked by the symmetry elements of the cell, and have identical, or mirror settings: the structure reduces to a one helix site cell.

elements of the unit-cell are 'used up' to generate the three helices, which are not therefore linked by any further element of symmetry. It is this very feature, clearly analysed by Puterman et al. [2], which enables the generation of different azimuthal settings for the three helices, i.e. of the frustrated packing scheme (Fig. 5*a*). In addition, the $P3_1$ (or $P3_2$) symmetry does not generate up and down helices at each helix site. Puterman et al. [2] were therefore led to give the coordinates of another repeat unit for every chain site in order to generate anticline helices. Note—and this will become important when discussing the crystal morphology—that the up- and down-helices thus created at any helix site are not (necessarily) related by any crystallographic element of symmetry. The repeat units defined for up and down helices must yield nearly isosteric helices, although such a substitution at one helix site was found to create steric problems.

Antiparallel helices are also created from three independent units when the space group is $P3_121$, by virtue of the two-fold axis. This space group has indeed been considered in the recent derivation of the crystal structure of βiPP by Meille et al. [7]. The two-fold axis creates a specific relationship between up- and down-pointing helices, as illustrated in Fig. 5*b*: the 'corner' (A) helix reproduces itself on the same site in up and down orientations (A and A′, the prime indicating anticlinicity), whereas B and C switch their locations on changing helix orientation (i.e. B and C′, and C and B′ are located at the same sites).

When, in the $P3_121$ space group, the repeat unit is defined as a full three-fold helix (Fig. 5*c*) [19,20] the two further helices have (in view of the 120° rotation) the same azimuthal setting as the initial helix (in addition to *c*/3 shifts) and therefore *do not* create a frustrated packing: actually, the cell thus obtained reduces to a simple one chain cell. In addition, three helices anticline to the previous ones are also generated: this space group therefore provides for the up–down statistical substitution. However, the azimuthal settings of up and down helices at each helix site are linked by the two-fold symmetry axis (Fig. 5*c*). Again, the structure reduces to a smaller unit-cell with one helix site, and does not account for the frustration.

From the above discussion, frustrated crystal structures based on three-fold isochiral helices are best described with the space group $P3_1$ or $P3_2$ (depending on helix chirality), and defining three monomer units (rather than a full helix) as the crystallographic repeat unit(s). Generation of oppositely oriented helices requires defining three additional monomer units. This is actually the (correct) procedure adopted by Puterman et al. [2] in their structure derivation of iP2VP. Generation of anticline helices via an additional two-fold axis as in the $P3_121$ space group imposes positional relationships between up and down helices which may not preserve the near-isostericity of up and down helices at each helix site.

4.1.3. Crystal growth and additional symmetries linked with twinning

Besides the impact expected from the symmetry of the unit-cell, additional apparent symmetries may be generated during crystal growth by twinning or microtwinning. Since we are dealing with a chiral structure, rotation twins are

most likely. However, reflection twins are also possible given the racemic nature of iP2VP. In view of the mirror symmetry involved, reflection twins change the space group from $P3_1$ to $P3_2$, and the twin plane is an antiphase boundary. Growth twins based on rotation twins have been documented in crystals of frustrated *chiral* polymers. They are easily identified, since the crystal morphology is affected. Existence of antichiral microdomains separated by antiphase boundaries is more difficult to detect: such domains have been identified in the α'' phase of syndiotactic polystyrene [21], and are at the root of significant streaking in the *hk*0 pattern of the β phase of isotactic polypropylene [6,7,22]. In both cases, the small scale 'microtwinning' manifests itself by a higher symmetry of the single crystals: they are hexagonal [6,7], whereas frustrated polymer structures are expected (and in many cases observed [9]) to have a triangular outline, or at least three-fold symmetry. For the present iP2VP, our attempts to find reflection twins or rotation twins have been unsuccessful: only a few growth twins have been observed, which do not display any clear cut crystallographic relationship between their constituant parts.

4.2. Morphology of iP2VP crystals and crystal symmetry

The above analysis of the iP2VP structure was purposely centred on crystal symmetry. Indeed, the crystal morphology illustrates several features of the crystal symmetry, some of which are expected, many others being novel.

4.2.1. Crystal symmetry, chain sense and helix settings

The morphology of iP2VP single crystals is characterized by the absence of any two-fold axis parallel to the plane of the crystal: in other words, as already indicated, the crystals are different if looked at 'from the top' or 'from the bottom'. Intuitively, such two-fold axes would however be expected for polymer crystals, since they correspond to the macroscopic manifestation of possible substitution at each helix site of anticline helices and to the equipartition between up and down helix orientations resulting from chain folding. One is therefore led to the uncomfortable necessity to reconcile a most probable *local* (at the unit-cell or even chain site level) up–down statistics with the absence of a macroscopic (at the level of the crystal) manifestation of this up–down substitution.

Morphological asymmetry may have two different origins: (i) Obviously, it may be related to the cell geometry. Indeed, a crystal with a triclinic or monoclinic unit-cell bound by (010) and (100) growth planes has a different shape when seen from the top or from the bottom, as a result of the different orientation of the β angle. (ii) Higher symmetry space groups (e.g. orthorhombic, tetragonal, trigonal, hexagonal), normally yield 'symmetric' single crystals. An asymmetry as observed in iP2VP indicates an asymmetry of the unit-cell *content* (as seen in chain axis projection): the crystal structure has no symmetry element such as two-fold or two-fold screw axis perpendicular to the *c* axis, or mirror or glide planes parallel to *c*. For iP2VP, this restriction imposes the $P3_1$ (or $P3_2$) space groups. This also implies that *the azimuthal settings characteristic of each iP2VP helix site must be maintained upon up–down substitution*, with only small adjustments of the setting angles (as schematized in Fig. 5*a*) to minimize the overall energy.

Low symmetries of the unit-cell are usually revealed, even for *symmetric* single crystals, by asymmetries of the diffraction patterns. Such asymmetries have been documented in the diffraction pattern of the α'' superstructure of syndiotactic polystyrene, which forms 'standard' hexagonal single crystals, and for which a frustrated structure has recently been established [22]: the asymmetry stems again from a common tilt of the constituting triplets relative to the (110) plane of the cell. A more spectacular example is illustrated by the square single crystals of modification III of isotactic poly(4 methyl-pentene-1) investigated by Pradère et al. [23] These authors observed that the diffraction patterns of different parts of the single crystals yield different, mirror symmetry related *hk*0 diffraction patterns. Dark field imaging revealed that the square crystals are actually made of many small microdomains in twin relationship (twinning by merohedry). The domains were considered to have the same molecular packing in the *ab* plane, but positioned in the crystal with opposite *c* axis directions. The possibility of right- and left-handed helices was mentioned. However, these data rather suggest that the space group of the tetragonal unit-cell of P4MP1 form III is of a type ($P4_1$ or $P4_2$, or $I4_1$, etc.) which have some characteristic (non zero) setting angle of the square helix projection relative to the *a* or *b* axes [24]. Such crystal structures can give rise to crystal domains with *different settings of the helices*. These domains are thus differentiated by this setting rather than by the relative *c* axis orientations (which, in all likelihood, are equal for the different domains) or (probably) helical hand.

Reverting back to iP2VP crystals, we note that the absence of a two-fold symmetry strongly suggests that they are not made of microdomains either isochiral (rotation twins) or antichiral (antiphase boundaries). Indeed, both twins would introduce a mirror symmetry (in chain axis projection) which is not observed.

4.2.2. Crystal symmetry, front, back and lateral growth rates

The frustrated nature of the structure also affects the growth rates, due to the different topologies of opposite sides of any crystallographic plane. Growth rates on opposite growth planes of the crystal are expected to differ: triangular crystals are often observed for frustrated structures [9]. Similarly, and in spite of their six-sided outline, iP2VP crystals have an overall three-fold symmetry. *The truly original feature*, not previously encountered even in triangular crystals of frustrated structures, is the development of growth faces which *are not normal to a radial*

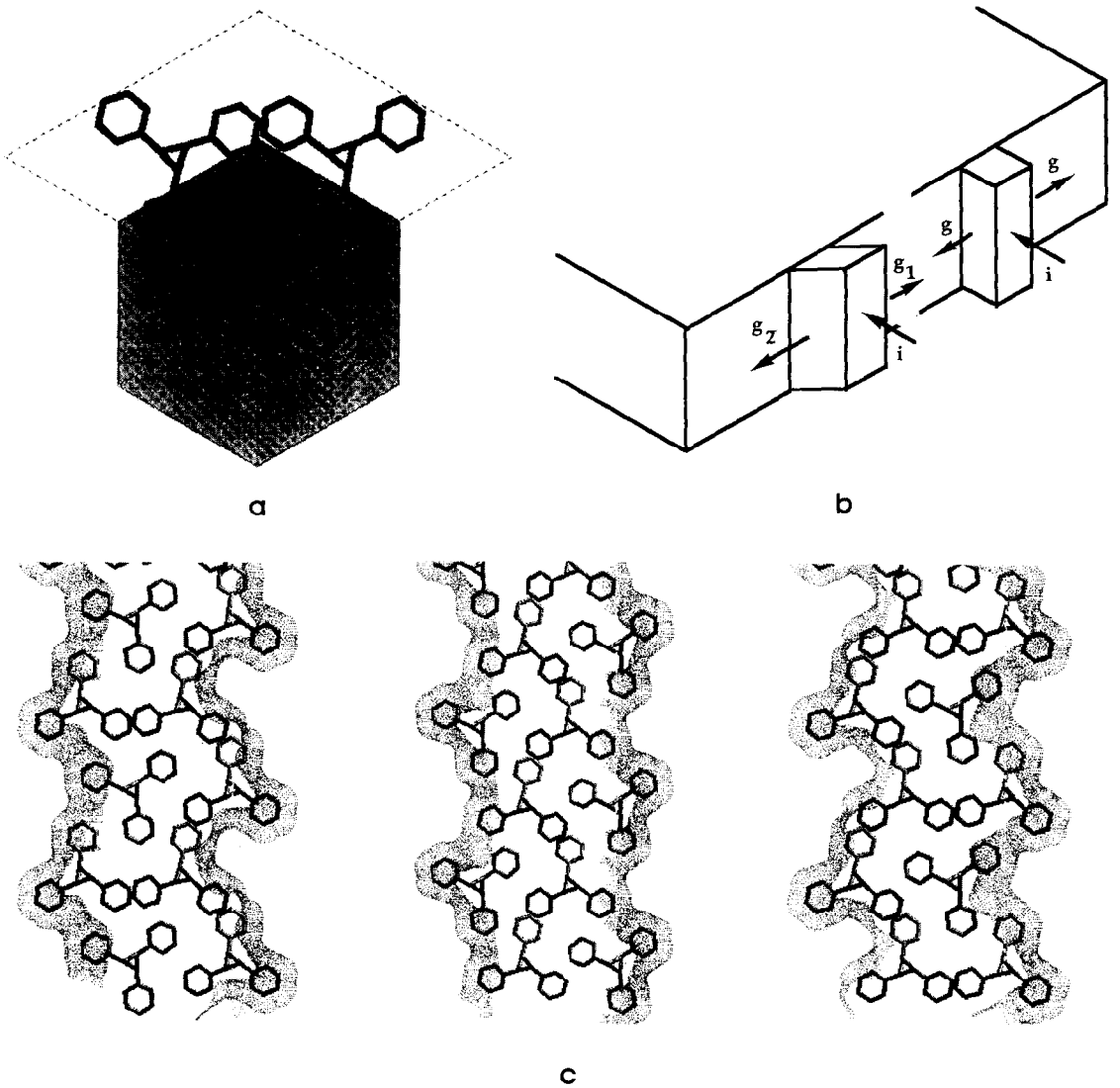

Fig. 6. (a) Hexagonal single crystal morphology predicted for crystals of iP2VP on the basis of its crystal structure by the 'morphology' module of Cerius [2] based on the Bravais–Friedel–Donnay–Harkar method. The calculated, hexagonal symmetry is higher than observed (cf. Fig. 2). (b) Illustration of the 'classical' picture (on the right-hand side of the drawing) of the initiation of a new growth layer by deposition of a stem (at a rate i) with a square section, and lateral spreads at a rate g. On the left-hand side, the growth mechanism suggested by the iP2VP crystal morphology: the deposition (at a rate i) is followed by unequal lateral spreads at rates g_1 and g_2 linked with different geometries of the deposition sites, either as a result of the geometry of the stems (triangular in this case) or of the substrate layer (cf. part (c)). (c) Topology of the (100) growth fronts of iP2VP. The Connally surfaces are shown for three crystal strips made of four layers, and shifted by one layer. The drawings therefore show the 'front' and 'back' surface of six (three in each direction) successive (100) growth layers of the structure. Note the relatively symmetric topologies of the right- and left-hand drawings, which correspond to the centre helices in Fig. 4*a*, and the lower symmetry of 'front' or 'back' growth fronts of the centre drawing.

growth direction. As already indicated, these faces should be (100), as anticipated from modelization of the crystal shape using the module of Cerius [2] (Fig. 6*a*). The tilt of the growth plane can only be interpreted by assuming *staggered* (100) growth planes in the face. This stagger suggests that, given one (primary) nucleation site on the (100) growth face, the lateral spreads of the newly formed layer (by deposition of secondary stems) are not equal. In other words, growth kinetics must distinguish *two different* lateral spreads g_1 and g_2, as illustrated schematically in Fig. 6*b*.

These differences in lateral spread rates result from *local asymmetries of deposition sites* in the growth face. As an illustration, the Connally surfaces of such growth faces are shown in Fig. 6*c*. They confirm that the front and back growth faces are different (if only slightly), which accounts for the fact that different growth rates are observed. Further, they indicate that the deposition sites have a 'polarity', i.e. cannot be approximated by a flat surface. However, whereas the molecular origin of the differences are understood, it is not, as yet, possible to discriminate between the two growth faces and to attribute a specific crystallographic 'side' of the (100) growth face to 'straight' and 'tilted' growth fronts. In any case, these observations highlight impacts of more local elements than usually considered in theories of crystal

growth (which usually assume a stem of square section deposited on a 'flat' substrate [25]), and illustrate aspects of polymer growth which are seldom accessible to experimental probing. Contrary to most crystals of frustrated structures which are triangular [9], the crystals of iP2VP have 'front' and 'back' growth rates close enough to reveal the additional and more interesting 'tilted' growth faces.

4.2.3. Crystal symmetry, crystal thickness and isothermal thickening

The differences in lamellar thickness of neighbour growth sectors further illustrate the intrinsic asymmetry of the frustrated structure. They arise however from two different phenomena: a possible, genuine initial thickness difference, and a noticeable impact of isothermal thickening.

The initial difference in lamellar thickness stems again from the different topologies of deposition sites illustrated in Fig. 6*c*. The energies of deposition of the incoming stem may differ widely depending on the topology of the deposition sites: upon deposition in a notch of the surface, one energy term $\sigma a l$ is regained since the two surfaces initially exposed reduce to one once the stem has filled the notch. The situation is more complex for frustrated structures. The *overall* (bulk) energy of crystallization must be the same on opposite (100) growth faces. However, the *partition* of this energy is different on opposite growth faces between the three successive layers which increment the growth front by one unit-cell. It is these 'sub unit-cell' differences which are responsible for the initial differences in lamellar thickness.

The initial differences in lamellar thickness are actually blurred (or enhanced) by a striking, sector-dependent isothermal lamellar thickening process. Its manifestations are best illustrated in Fig. 2*b* and Fig. 3: the 'tilted' (100) growth sectors are thicker, their fold surface is smoother than the 'straight' (100) growth sectors, and they display curved corrugations. The analysis of these morphological features is helped by available experimental evidence on lamellar thickening of single crystals of poly(ethyleneoxide) (PEO).

PEOs of low and medium molecular weight ($\approx$ 3000–10 000) crystallize from the bulk in the form of lamellar crystals, the thickness of which is a sub-multiple of the molecular length. Depending on crystallization temperature, the chains are either extended, or once, twice, etc. folded [26]. Kovacs and Straupé [27] and later Cheng and Chen [28] have investigated in much detail the growth kinetics of these crystals. The experimental procedure rests on isothermal growth of single crystals in thin films, and quenching of the samples in a cold bath to arrest growth. A typical morphology of such a crystal is shown in Fig. 7*a*, and its analysis is given in Fig. 7*b*.

The crystal grows initially in the form of once folded chains from an extended chain nucleus (produced by self-seeding). While growth of the once folded chains proceeds,

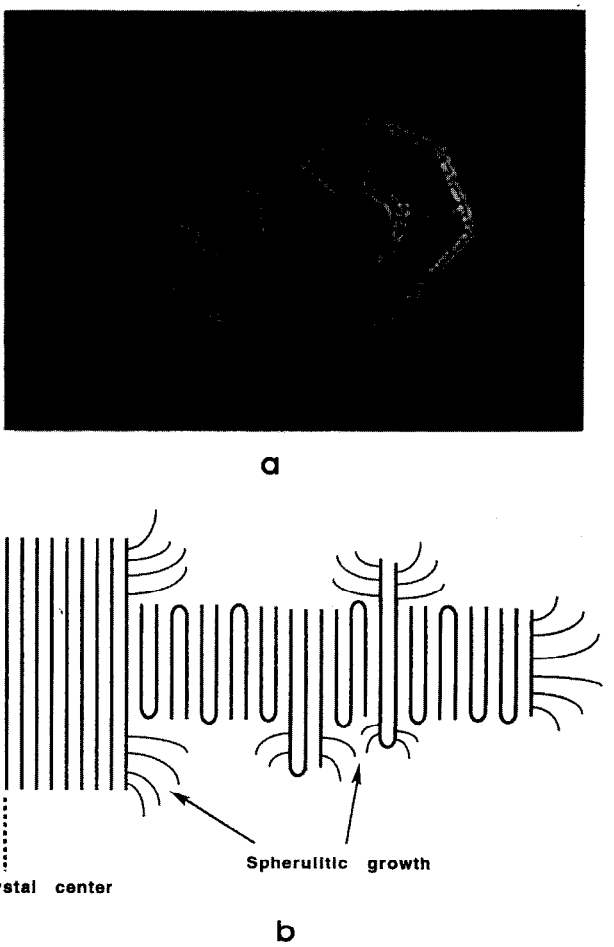

Fig. 7. (a) Melt grown single crystals of polyethylene oxide produced by Kovacs and Straupé[27]. The crystals are grown at high T_c and quenched. Optical micrograph, crossed polars. (Reproduced from [27], with permission.) (b) Schematic drawing illustrating the nucleating activity of protuberances at the surface of lamellar crystals and the resulting birefringence observed in part (a), as opposed to the absence of nucleation in smoother, thickened parts at the centre of the crystals.

a mechanism of lamellar thickening sets in, starting from the central, extended chain nucleus. This thickening (to chain extended lamellae) implies unfolding of chains already present in the crystal, and dragging in of molecules from the surrounding melt. Kovacs and Straupé [27] noted early on that the surface of the once-folded part of the crystals was more 'decorated' on quenching by additional growth than the extended-chain part. This higher density of decoration indicates that the extended chain parts of the crystals have a 'smooth' surface, whereas protrusions exist in the once-folded part of the lamellae, which nucleate spherulitic growth on cooling, as schematized in Fig. 7*b*.

The features displayed by the different growth sectors of iP2VP crystals parallel in many respects those already analysed for PEO crystals:

1. The 'straight' (100) growth sectors do not thicken (or thicken to a very limited extent). They have a very rough surface, which can be visualized by EM and

AFM since, due to the slow growth rates of iP2VP, they have not nucleated additional growth on cooling. If we assume that thickening has a marginal effect, then lamellar growth produces initially very irregular lamellar surfaces, with differences in stem lengths well beyond the $\approx$ 10 nm range (from the shadow length).

2. In 'tilted' (100) growth sectors, isothermal lamellar thickening 'smooths out' the lamellar thickness and, at the same time, provides a rational explanation for the curved corrugations seen in Fig. 2*b*. We recall that the central part of the corrugations is bent inwards, but remains parallel to the (100) growth planes, whereas the outer parts are bent towards the growth sector boundaries. These features suggest that, in the thickening process, the number of growth layers decreases, due to the insufficient compensation of the 'incoming' molecules sucked in the crystal from the surrounding melt (this effect may be due to a depletion of available material, as a result of the thin film morphology used in our experiments). Due to this insufficient compensation, the overall number of growth planes decreases from its initial value, which should result in a global shrinkage of the crystal. However, the number of growth layers is not reduced at the growth sector boundaries, which are 'pinned' by the dimensional stability of the neighbour sectors (since they do not experience the same lamellar thickening)—thus the apparent overall inward bending of the corrugations.

Whereas the manifestations of lamellar thickening can be analysed with reasonable confidence, the link between these different behaviours and the crystal structure, or more precisely the local arrangement of stems in the crystals cannot be made at this stage. Indeed:

1. The different behaviours could reflect a genuine difference in the crystal structure, for example the coexistence of the two different frustrated packing schemes NWW and NSS. We have taken diffraction patterns from the different growth sectors, but observed no differences in relative intensities of the *hk*0 spots to support this hypothesis.
2. The different behaviours may be linked with the initial lamellar thicknesses in the growth sectors. However, the significantly different behaviours would suggest a 'threshhold' lamellar thickness beyond which lamellar thickening could take place (not to mention the more complex thickening behaviours uncovered for PE and PEO [25] in case of initial non-integral folding).
3. A possible explanation may involve a (as yet undetermined) interplay of crystal structure and pattern of chain folding. For example, according to Puterman et al. [2], substitution of an up- by a down-pointing helix is difficult at one helix site at least, which may impose restrictions on relative orientations of stems, and therefore on chain folding around this 'difficult' location. Such restrictions can be viewed as a second frustration, additional to, but independent from, the crystallographic frustration considered so far.

5. Conclusion

The crystal morphology of iP2VP is highly unusual in polymer science. Its analysis provides insights into the correlation between crystal morphology and the specificities of frustrated polymer structures, and highlights features of more general relevance on polymer crystal growth. It has been shown that:

1. Single crystals of iP2VP have six growth faces, but three-fold symmetry: *the crystals have a polarity* since they are different when seen 'from the top' or 'from the bottom'. These features are fully consistent with, and explained by the lack of symmetry of their frustrated packing of three-fold helices. They are only compatible with the $P3_1$ (or $P3_2$) space group correctly determined by Puterman et al. [2], thus excluding the $P3_121$ space group sometimes used to describe frustrated structures. The crystals are probably chiral, i.e. do not include antiphase boundaries between domains made of helices of opposite hand, in spite of the racemic molecular configuration of iP2VP.
2. Three thin sectors bound by 'straight' (100) growth faces alternate with thicker sectors with 'tilted' growth faces. These features indicate a strong impact of local aspects of crystal growth, which are brought to light by the asymmetry of the frustrated packing: unequal growth rates of completion of growth faces once the initial stem is deposited, uneven partition of the overall energy of crystallization between the three depositing stems.
3. iP2VP single crystals provide a very illustrative example of lamellar thickening, since alternate growth sectors are affected differently. Non-thickened growth sectors have a rough fold surface, probably representative of the initially formed crystal. Isothermal thickening results in considerable lamellar rearrangements, including smoothening of the fold surface (i.e. equalization, as well as increase of the fold length) and, under the thin film growth conditions used in the present study, decrease of the initial number of growth planes. The structural origin of these different responses to isothermal thickening lie again in the asymmetry of the frustrated packing, although it is difficult to pinpoint which specific novel aspect of the structure is involved.

Acknowledgements

We wish to thank Ms Sabine Graff for the AFM examination of the single crystals, and Prof. J. J. Point (Université de Mons) for helpful discussions.

References

[1] Alberda van Ekenstein GOR, Tan YY, Challa G. Polymer 1985;26:283.
[2] Puterman M, Kolpak FJ, Blackwell J, Lando JB. J Polym Sci Polym Phys 1977;15:805.
[3] Toulouse G. Commun Phys 1977;2:115.
[4] Syozi I. In: Domb C, Green MS, editors. Phase transitions and critical phenomena London: Academic Press, 1972:269.
[5] Lotz B, Kopp S, Dorset D. C R Acad Sci Paris 1994;319:187.
[6] Dorset D, McCourt M, Kopp S, Schumacher M, Okihara T, Lotz B. Polymer, submitted.
[7] Meille SV, Ferro DR, Brückner S, Lovinger A, Padden FJ. Macromolecules 1994;27:2615.
[8] Cartier L, Spassky N, Lotz B. C R Acad Sci Paris 1996;322:429.
[9] Cartier L, Okihara T, Lotz B. Macromolecules 1997;30:6313.
[10] Keller A. Rep Progr Phys 1968;31:623.
[11] Cartier L, Spassky N, Lotz B. Macromolecules 1998;31:3040.
[12] Cartier L, Lotz B. Macromolecules 1998;31:3049.
[13] Natta G, Corradini P, Bassi W. Nuovo Cimento 1960;15(Suppl):69.
[14] Natta G, Corradini P, Bassi W. Nuovo Cimento 1960;15(Suppl):57.
[15] Corradini P, Bassi IW. J Polym Sci, Part C 1968;16:3233.
[16] Meille SV, Allegra G. Macromolecules 1995;28:7764.
[17] Brückner S, Meille SV, Petraccone V, Pirozzi B. Prog Polymer Sci 1991;16:361.
[18] Sen Y, Lotz B, et al, to be submitted.
[19] Matsubayashi M, Chatani Y, Tadokoro H, Dumas P, Spassky N, Sigwalt P. Macromolecules 1977;10:996–1002.
[20] Sasisekharan V. Acta Cryst 1959;12:903–909.
[21] Pradere P, Thomas EL. Macromolecules 1990;23:4954.
[22] Cartier L, Okihara T, Lotz B. Macromolecules 1998;31:3303.
[23] Pradère P, Revol JF, St John Manley R. Macromolecules 1988;21:2747.
[24] De Rosa C, Borriello A, Venditto V, Corradini P. Macromolecules 1994;27:3864.
[25] Hoffman JD, Davis GT, Lauritzen Jr JI. In: Hanney NB, editor. Treatise on solid state chemistry, vol 3 New York: Plenum Press, 1976:541.
[26] Arlie JP, Spegt P, Skoulios A. Makromol Chem 1966;99:160; 1967;104:212; Spegt P Makromol Chem 1970;140:167.
[27] Kovacs AJ, Straupé C. J Crystal Growth 1980;48:210.
[28] Cheng SZD, Chen J. J Polym Sci, Polym Phys Ed 1991;29:311.